Placement Optimization for UAV-Enabled Wireless Networks with Multi-Hop Backhauls in Urban Environments

Sining Yang
National University of Defense Technology, NUDT
Changsha, China
yangsining16@nudt.edu.cn

Dianxi Shi
Defense Innovation Institute, Tianjin Artificial Intelligence Innovation Center, NUDT
Beijing, Tianjin, Changsha, China

Yingxuan Peng
NUDT
Changsha, China

Shaowu Yang
NUDT
Changsha, China

Bo Zhang
Defense Innovation Institute
Beijing, China

Wenjing Yang*
NUDT
Changsha, China
wenjing.yang@nudt.edu.cn

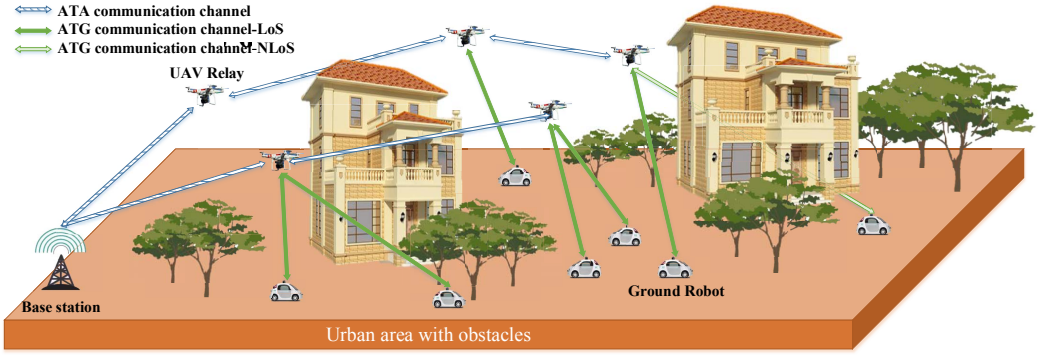

Figure 1: The urban surveillance or post-disaster scenario, where several ground robots survey it in predefined ways and transmit collected data to a remote base station via a UAV-enabled wireless multi-hop network. Due to the existence of obstacles, ATG communication links may have LoS or NLoS propagations.

ABSTRACT

In surveillance or search scenarios, exploiting unmanned aerial vehicles (UAVs) as relays to provide wireless data access for task-oriented ground robots (GRs) with remote base station have emerged as a promising application. This paper considers a UAV-enabled wireless network, where communication links could be line-of-sight (LoS) and non-line-of-sight (NLoS) due to obstacles in urban environments. Existing works typically adopted the free-space path loss model or the statistical channel model, which either ignored the impact of obstacles or assumed uniformly distributed obstacles and therefore might fail in practical NLoS scenarios. In this paper, taking the information of randomly distributed obstacles in environments into consideration, we aim to optimize the placement for the UAV-enabled multi-hop network to transfer more data collected by GRs and minimize the time delay in data transmission while satisfying the required communication quality. By reconstructing this complex non-convex optimization problem into two subproblems and solving them alternatively, we propose the multi-hop UAVs placement (mUP) method to get the solution, which contains the air-to-ground network formation (ATG-NF) algorithm and the communication quality-aware UAV placement (CQA-UP) algorithm. Simulation results show that in four types of typical urban environments or with different numbers of UAVs, the proposed mUP method achieves substantial performance gains in terms of communication quality and task performance compared to other placement approaches based on statistical channel models. We further discuss the robustness of the mUP method towards terrain measurement error.

KEYWORDS

Unmanned aerial vehicle (UAV), communication quality-aware, wireless networks, multi-hop backhauls, placement optimization, surveillance, post-disaster, urban environments, LoS propagations, NLoS propagations, randomly distributed obstacles

1 INTRODUCTION

The dense deployment of small base stations is one of the typical features of the emerging 5G networks. However, in post-disaster search and rescue scenarios or surveillance scenarios, backhaul access is usually either unavailable or limited in capacity [10]. Due to the unmanned aerial vehicles (UAVs) have swift mobility, flexible deployment capabilities and relatively high possibility to establish line-of-sight (LoS) communication links with ground robots (GRs), exploiting UAVs as relays to enable multi-hop wireless backhaul

*Corresponding author: Wenjing Yang.

978-1-6654-9624-7/22/$31.00 ©2022 IEEE
DOI 10.1109/IPSN54338.2022.00012

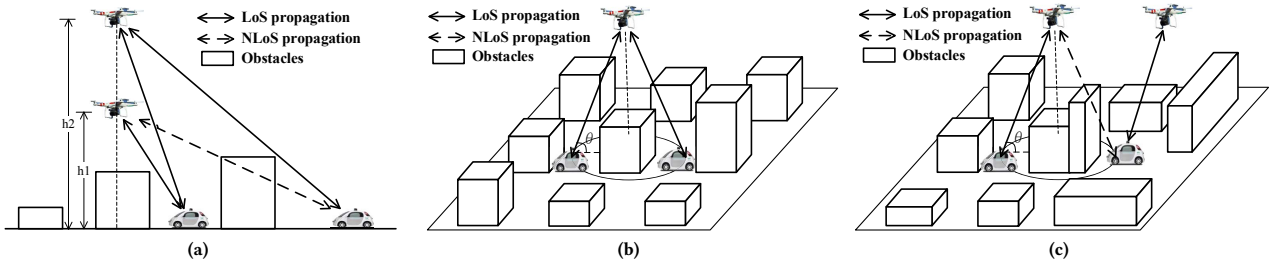

Figure 2: Widely-used communication channel models and their limitations. (a) The free-space path loss model may hold true when the UAV flies sufficiently high that GRs are unlikely blocked by local obstacles, which however may lead to a communication performance bottleneck. (b) In the statistical channel model, obstacles are assumed to be uniformly distributed. Furthermore, the probability of each ATG link having LoS propagation depends on distribution-related parameters and elevation angle at GR. (c) In realistic urban environments with randomly distributed obstacles, solutions based on the statistical channel model may fail at some locations.

networks for task-oriented GRs with the remote base station (BS) is a promising application [15, 20]. Since the existence of obstacles in urban environments would result in damaged communication quality and therefore lead to poor task performance, one of the major challenges in the UAV-enabled multi-hop wireless communication scene in urban environments is how to deploy UAVs to transfer more data collected by GRs and minimize the time delay with communication quality constraints satisfied [10, 13, 14, 21].

Several studies have been devoted to this challenge. Considering the free-space path loss model, authors in [12] optimized bandwidth, power allocation, and position deployment of UAVs by alternating optimization and successive convex programming (SCP) to maximize the throughput of the UAV-enabled network. In a similar cellular-connected UAVs-enabled network, by adopting the Rayleigh fading channel model, authors in [4] considered a tradeoff between maximizing energy efficiency and minimizing the communication interference and wireless latency, and proposed a deep reinforcement learning algorithm to solve it. However, communication channel models that these works adopted have ignored the impact of obstacles and can only hold true in scenarios where the UAV flies sufficiently high that GRs are unlikely blocked by local obstacles, such as trees and buildings. In this case, as shown in Fig. 2a, high flying altitude ($h_2 >> h_1$) may lead to the communication performance bottleneck caused by path loss [1, 13].

Some other existing works adopted the statistical channel model to design the multi-hop backhaul network [3, 8, 17, 18]. Exploiting the framework of network formation games, the authors proposed a myopic network formation algorithm to maximize the utility function considering the achievable data rate, wireless latency [3, 17], and energy consumption [18] comprehensively. In [8], the authors proposed a novel hybrid 5G Fiber-Wireless access architecture and proposed genetic algorithms to maximize the number of the served users within latency constraints. Among these works, the statistical channel model is based on the assumption that obstacles are uniformly distributed; therefore the probability of each air-to-ground (ATG) link having LoS propagation depends on distribution-related parameters and elevation angle at each GR, as shown in Fig. 2b. However, in realistic urban environments with randomly distributed obstacles, solutions based on them may fail at some locations. For example, as shown in Fig. 2c, the resulting relay position theoretically can experience LoS propagation while actually may utilize the non-line-of-sight (NLoS) propagation and lead to damaged communication quality. This is because the actual position and shape information of obstacles are not well used.

Such being the case, some other researchers proposed some methods to use the information of obstacles to plan the position of UAV relay [5, 11, 19]. Based on fine-grained LoS information, the authors in [5] proposed an efficient algorithm to arrange the position of UAV relay to maximize end-to-end throughput. Similarly, in [7], the authors proposed a positioning algorithm to smartly place a UAV relay to improve the connectivity in a wireless mesh network. Considering the effects of LoS obstructions in urban areas, the authors in [11] proposed a learning approach to predict ATG communication strength to plan the trajectory of UAV relay. Besides, in [19], the authors considered the information of obstacles in environments and proposed an LoS condition-based division method to solve a concave optimization problem to arrange the energy-efficient trajectory of the UAV relay. Note that a multi-robot system can significantly extend the service areas and improve the task-performing efficiency by cooperation. However, the above researches only considered one UAV relay, which left the placement of a multi-hop UAV-enabled network considering communication quality constraints relatively unexplored.

This thus motivates our current work to investigate the placement optimization of the UAV-enabled multi-hop network in urban areas, which considers the information of obstacles in environments. As shown in Fig. 1, we consider an urban surveillance scenario, where communication links could be LoS and NLoS due to obstacles in environments. Several GRs survey an urban area in predefined ways and transmit collected data to the remote base station via a UAV-enabled wireless backhaul network. We aim to form an optimized placement of UAVs to maximize the amount of transferred data and minimize the time delay while maintaining the required communication quality.

To our best knowledge, *this is the first work that takes randomly distributed obstacles into consideration to design a UAV-enabled multi-hop backhaul network to satisfy the required communication quality in urban environments*. The main contributions of this paper are summarized as follows.

- Considering environments with many obstacles, we adopt the signal-to-noise ratio-based (SNR-based) communication channel model, which captures both LoS and NLoS propagations. Furthermore, we propose a multi-hop UAVs placement (mUP) method to form a UAV-enabled wireless network aiming at transferring more data and minimizing the time delay.
- The mUP problem is reconstructed into the ATG network formation subproblem and the communication quality-aware UAV placement subproblem, and be solved alternatively. We design a UAV-UAV game and a GRs-network game and incorporate the virtual force field (VFF) to solve the first subproblem to get the topology of the network. Then based on the information of obstacles in environments, we propose a communication quality-aware UAV placement algorithm to ensure UAVs are placed in positions where communication qualities between UAVs and linked GRs are satisfied.
- Numerical results demonstrate that the proposed mUP method achieves substantial communication quality and task performance improvement in four typical urban environments or with different numbers of UAVs compared with methods that only use VFF and adopt the statistical channel model. Our mUP method can ensure that 80% of ATG links are valid while up to 50% of links generated by the other two methods are blocked by obstacles. Besides, Our mUP method can transfer up to 2 times the amount of data as much as these two methods. In addition, simulation results show that the mUP method can be applied in successive task executions in surveillance scenarios. We further discuss the robustness of the mUP method towards terrain measurement error.

The rest of this paper is organized as follows. At first, we present the SNR-based communication channel model and formulate the mUP problem in Section 2. Then, the mUP method is given in Section 3. Simulation results are provided and analyzed in Section 4. At last, we draw conclusions in Section 5.

2 SYSTEM MODEL AND PROBLEM FORMULATION

We consider a wireless multi-hop network composed of one base station, a set $\mathcal{N}$ of N UAVs, and a set $\mathcal{M}$ of M GRs in post-disaster search and rescue scenarios or surveillance scenarios in urban environments. Due to disasters, terrestrial wireless infrastructures are damaged, and we place one BS on the rooftop that is higher than all buildings. GRs with different acquisition capabilities execute their tasks (collect interested data) in street levels in predefined ways. Besides, we assume that all UAVs fly at the same altitude which is higher than obstacles, as commonly done in prior works [3, 5]. Due to the existence of obstacles in environments, a ground backhaul network connecting GRs to the BS is either limited in capacity or significantly obstructed. Therefore, we consider a UAV-enabled wireless multi-hop network to overcome the bottleneck that provides GRs with the BS wireless data access.

Note that UAV-to-GRs data links can be obstructed due to obstacles surrounding the GRs. And UAV relays cannot be placed too close to some specific GRs since they need to strike a balance between ensuring at least one UAV has access to BS, transmitting more data collected by GRs, and reducing time delay in data transmission. To address this dilemma, we aim to optimize the placement of UAVs to transmit more data collected by GRs and reduce time delay in this paper. Key notations are summarized in Table 1.

2.1 SNR-based Communication Channel Model

The prediction of communication quality is of great significance to the optimization of UAV deployment. Considering a classic wireless communication channel model consisting of pathloss and shadow fading, we use the received SNR as the performance metric to characterize wireless communication quality. And SNR between the transmitter i and receiver j can be given by

$$SNR_{ij} = P_i / {d_{ij}}^{\beta} N_0 B \Psi_{ij}, \tag{1}$$

where P_i represents the transmit power of i, d_{ij} is the Euclidean distance between i and j, β refers to the pathloss exponent, N_0 (W/Hz) represents the power spectral density of the additive white Gaussian noise (AWGN), B (Hz) is the channel bandwidth, and Ψ_{ij} represents the shadow fading component accounting for diffraction and multipath fading between i and j. The Doppler effect caused by the mobility of UAVs is assumed to be completely compensated as done in [4]. Besides, Ψ_{ij} (dB) follows the Gaussian distribution and can be expressed as [11]:

$$\begin{cases} \Psi_{ij}^{\mathrm{LoS}} \sim \mathcal{N}(\mu_{ij}^{\mathrm{LoS}}, (\sigma_{ij}^{\mathrm{LoS}})^2), & \text{LoS propagation,} \\ \Psi_{ij}^{\mathrm{NLoS}} \sim \mathcal{N}(\mu_{ij}^{\mathrm{NLoS}}, (\sigma_{ij}^{\mathrm{NLoS}})^2), & \text{NLoS propagation.} \end{cases} \tag{2}$$

In (2), μ_{ij} and σ_{ij}^2 refer to mean and variance respectively, and can take either of two values for cases of LoS and NLoS propagations.

In our system model, communication links contain the air-to-air (ATA) links between UAVs and UAVs (or BS), and ATG links between UAV and GRs. For the ATA links, we assume that UAVs fly higher than obstacles, so that ATA wireless channels are dominated by LoS links [3, 6, 8] and the shadow fading component can be expressed by Ψ_{ij}^{LoS}. For ATG links, in urban environments, LoS and NLoS propagations both should be considered.

Besides, to overcome the co-channel interference among different GRs and UAVs, orthogonal transmission in the time domain among different ATG and ATA links is considered, which means we use time-division multiple access (TDMA) in this paper. In other words, each link is assigned with a dedicated data transmission time slot. In addition, we can reduce the overhead of synchronization by applying methods like delay-tolerant synchronization approach [16].

2.2 The mUP Problem Formation

As shown in Fig. 3, the UAV-enabled multi-hop network can be represented as an undirected graph $G(V, E)$, where V represents the set of all vertices (N UAVs, M GRs and one BS) and E represents the set of all communication links. Similar to [3], we consider a network with bidirectional tree structure rooted at BS o, which allows each UAV/GR to connect to BS via at most one path. The

Table 1: Key notations

Symbols	Meaning
$\mathcal{N}, \mathcal{M}$	The sets of UAVs and GRs separately, $\mathcal{N} \triangleq \{1, 2, ..., N\}$ and $\mathcal{M} \triangleq \{1, 2, ..., M\}$.
x_{Un}, x_{GR_m}	The positions in three dimensional of the UAV U_n and the GR GR_m separately.
SNR_{ij}	The signal-to-noise ratio (SNR) between the transmitter i and receiver j.
Ψ_{ij}	The shadow fading component accounting for diffraction and multipath fading between i and j.
$G(V, E)$	An undirected tree-structured graph, with V representing the set of all vertices and E being the set of all communication links.
a_m (bits/s)	Data acquisition rate of each GR GR_m.
A_n (bits)	The total amount of data should be transferred by U_n, which comes from its links GRs and its child UAVs.
$t_{o,n}, t_{nm}, t_{nn'}, t_{n''n}$	The time slots between BS o and UAV U_n, UAV U_n and GR GR_m, UAV U_n and its child UAV $U_{n'}$, and UAV U_n and its parent UAV $U_{n''}$ separately ($n, n' \in \mathcal{N}, m \in \mathcal{M}, n \neq n', n''$).
t_{delay_m}	The time delay in data transmission of one GR m.
$p(n), c(n)$	The parent node of UAV U_n and child nodes of UAV U_n separately, in the tree-structure network G.
ρ_n	The set of UAVs, which are parent nodes of U_n from BS to itself, $\rho_n = \{U_{l1}, U_{l2}, ..., U_{ln}\}$ ($p(l1) = BS, U_{ln} = U_n$).
$e_{nn'}, e_{nm}$	ATA communication link between UAV U_n and another UAV $U_{n'}$, and ATG communication link between UAV U_n and GR GR_m.
$G - e_{nn'}, G + e_{nn'}$	Deleting and adding link $e_{nn'}$ from G separately.
$dis(U_n, U_{n'}), dis(U_n, c(n))$	The Euclidean distances between UAV U_n and another UAV $U_{n'}$, and between UAV U_n and its child UAV $c(n)$ separately.
GR_{U_n}	Directly linked GRs with UAV U_n ($n \in \mathcal{N}$).
$O(x, dia)$	A circle with its center is x and diameter is dia.
$D_{x_{U_i}}, S(D_{x_{U_i}})$	The domain of x_{U_i} and its area.

tree-structure network topology constraint can be formulated as follows:

$$\begin{cases} \sum\limits_{n \in \mathcal{N}} \Phi(t_{no}) \geq 1, \\ \sum\limits_{n \in \mathcal{N}} \Phi(t_{nm}) \leq 1, \\ \sum\limits_{n, n' \in \mathcal{N}, n \neq n'} (\Phi(t_{no}) + \Phi(t_{nn'})) = N. \end{cases} \tag{3}$$

In (3), $\Phi(t)$ is an indicator function taking value 1 if time $t > 0$, and 0 otherwise. $\Phi(t)$ can also be regarded as a mapping function which maps the time slot allocation into network topology. In other words, if a time slot is allocated between UAV U_n ($n \in \mathcal{N}$) and UAV $U_{n'}$ ($n' \in \mathcal{N}$) ($t_{nn'} > 0$), there exists a communication link between them ($\Phi(t_{nn'}) = 1$). Besides, in (3), the first constraint ensures that at least one UAV U_n is connected to BS o, the second constraint guarantees that each GR GR_m is connected to at most one UAV U_n, while the third constraint guarantees the number of formed edges in the network is the same as that of UAVs. Therefore, (3) guarantees the tree-structure network topology.

As shown in Fig. 4, we quantize task execution time into multiple time intervals. Each time interval contains two stages. In stage I, GRs collect interested data in predefined ways, and UAVs are deployed according to our proposed mUP method. In stage II, UAVs and GRs both arrive at predefined or planned positions, where they are motionless or in hovering to transfer data from GRs to BS via UAVs relay. The transferred data include the collected data (like images, audios) and destinations of GRs in next time interval. In addition, time of stage I (t_I) is fixed while time of stage II (t_{II}) depends on data transmission time, which can also be called time delay and is part of our optimization objective.

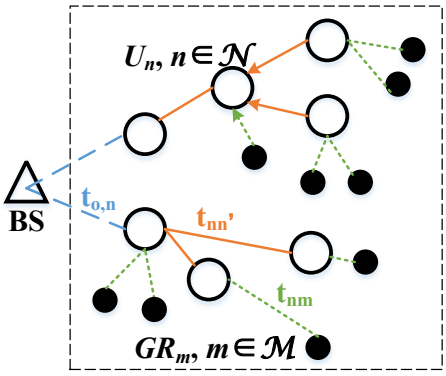

Figure 3: Illustration of the tree-structure network composed of N UAVs and M GRs, which rooted at BS.

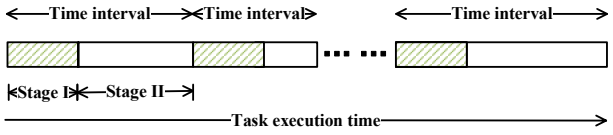

Figure 4: Illustration of the task execution time, which is quantized into multiple time intervals. Each time interval contains two stages: stage I is the GRs data collection and UAVs placement stage, while stage II is the data transmission stage.

Time delay in data transmission relates to the amount of data to be transferred. Speaking of the amount of data to be transferred,

we assume GRs could carry different kinds of sensors, such as image, audio, humidity sensors, to satisfy different task requirements. Therefore, acquisition capabilities of GRs could be different. For each GR GR_m, it can collect $a_m t_I$ (bits) data during one time interval. Given the spectral efficiency of the UAV relay S_U (bit/s/Hz), the time for these data to be transmitted by a UAV relay can be expressed as $t_m = a_m t_I/(BS_U)$. Besides, as shown in Fig. 3, one UAV U_n has to transfer data coming from not only directly linked GRs but also child UAVs, the amount of which is denoted by A_n. Then, the time slot constraint (each time slot allocated to each link should be long enough for U_n to transmit related data) can be represented as:

$$S_U t_{n''n} B \geq \sum_{\substack{n' \in N \\ n' \neq n, n''}} \Phi(t_{nn'}) A_{n'} + \sum_{m \in M} \Phi(t_{nm}) A_m, \forall n. \quad (4)$$

To formulate the time delay, we first define path pa_l from leaf node (UAVs with no child UAVs) $U_l, (l = 1, 2, \ldots, L)$ to the BS o as $pa_l = U_{l1}U_{l2}...U_{lk}U_{lk+1}...U_{lK}, k \in \mathcal{K}$, where $\mathcal{K} \triangleq \{1, 2, ..., K-1\}$, $U_{l1} = U_l, U_{lK} = o$, and each link $e_{U_{lk}U_{lk+1}} \in E$. Then, the time delay in data transmission of GR_m over path pa_l can be represented as $t_{delay\_m} = t_{m,l1} + \sum_{k \in \mathcal{K}} t_{lk,lk+1} + t_{lK,o}, \forall m$.

For notational convenience, we define $T = \{t_{nn'}, t_{nm}, t_{on}, \forall m, n, n', n \neq n'\}$. Our objective is to optimize the placement of UAVs to transmit more data collected by GRs in less time delay, which can be formulated as:

$$\begin{aligned} \min_{T, x_{Un}, n \in \mathcal{N}} \quad & J = \omega \sum_{m \in M} t_{delay\_m} - \sum_{n \in N} \sum_{m \in M} \Phi(t_{nm}) A_m \\ s.t. \quad & \frac{\Phi(t_{nn'}) P_n}{N_0 B d_{nn'}{}^{\beta} \Psi^{\text{LoS}}} \geq SNR_{\min}, \\ & \frac{\Phi(t_{nm}) P_n}{N_0 B d_{nm}{}^{\beta} \Psi_{nm}} \geq SNR_{\min}, \\ & \frac{\Phi(t_{no}) P_n}{N_0 B d_{no}{}^{\beta} \Psi^{\text{LoS}}} \geq SNR_{\min}, \\ & dis(U_n, U_{n'}) > d_{\text{safe}}, \forall n, n', m, n \neq n', \\ & (3) \text{ and } (4). \end{aligned} \quad (5)$$

In (5), ω is a tradeoff parameter which can weigh the importance between transferring more data and minoring time delay in data transmission. And the first three constraint functions are SNR-based communication links constraints according to (1), in which $SNR_{\min}$ denotes the minimum threshold of required SNR to transmit reliably. And $SNR_{\min}$ is determined by modulation method, coding rate and communication rate [3]. The fourth constraint function is the physical collision avoidance constraint, which means the distance between different UAVs should be no closer than the safe distance d_{safe}. Besides, the problem also subjects to the tree-structure network topology constraint in (3) and the time slot constraint in (4).

3 MULTI-HOP UAVS PLACEMENT METHOD DESIGN

This section aims to solve the mUP problem (5), which is complex due to the multiple optimization variables and nonconvex nature caused by obstacles. As given in Algorithm 1, we tackle the problem by reconstructing it into two simpler subproblems and solving them alternatively. *The first subproblem is constructed as an ATG network formation (ATG-NF) problem.* In the first subproblem, we suppose positions of UAV relays are in domain where all links with GRs are LoS, and the goal is to find the optimal data transmission time slot T^* (also can be deemed as the topology of the network) to maximize the amount of transmitted data and minimize time delay. Then, upon solving the first subproblem, *the second subproblem can be reformulated as a communication quality-aware UAV placement (CQA-UP) problem.* In the second subproblem, for all possible positions of UAVs, the optimal topology of the network are given by T^*, and the goal of the second subproblem is to find positions of UAVs to ensure required communication quality while maximizing the amount of transmitted data and minimizing time delay.

Algorithm 1 The mUP Algorithm

Input: Network G (initialized as a star network or resulted tree-structure network in last time internal), GRs, $\mathcal{N}$, obs (information of obstacles).

while G has not yet converged **do**
  Pick U_n ($n \in \mathcal{N}$) according to the assigned priority sequentially.
  U_n activate another $U_{n'}$ ($n' \in \mathcal{N}, n \neq n'$) randomly but uniformly.
  Pick all unlinked GRs as $unGRs$. Cluster $unGRs$ based on positions, pick the set with the maximum amount of data as $tarGRs$.
  ATG-NF(G,U_n,$U_{n'}$,$tarGRs$**)**.
  Define linked GRs with U_n as GR_{U_n}.
  if $GR_{U_n} \neq \varnothing$ **then**
    Pick parent nodes of U_n from BS to itself as $\rho_n = \{U_{l1}, U_{l2}, ..., U_{ln}\}$ ($p(l1) = BS, U_{ln} = U_n$).
    CQA-UP(ρ_n,obs,$tarGRs$,$\mathcal{N}$**)**.
  end if
end while
return resulted network G

3.1 ATG Network Formation Problem

If all ATG links are LoS, the problem (5) can be constructed as an ATG-NF problem. The goal is to form an aerial multi-hop backhaul network that allows each UAV to be connected to the BS via one path and connects as many GRs as possible via fewer hops. For the network formation problem, a framework of network formation game was proposed in [3, 17], where each UAV was an independent decision player to take action aiming at optimizing its utility function, and the result of the game was the graph G allowing all UAVs to be connected to the BS. However, in this framework, users at ground level were considered as a whole and were in one-to-one correspondence with UAVs, which might fail to satisfy the demands of the wireless communication quality between some GRs and UAVs due to the existence of obstacles. Therefore, apart from the formation of aerial network between UAVs, the connection between GRs and UAVs should also be considered, which together constitutes the ATG-NF problem. The proposed ATG-NF algorithm contains two games design and VFF incorporation.

3.1.1 The UAV-UAV game and the GRs-network game. We design two games to get the topology of the ATG network, which is the UAV-UAV game and the GRs-network game. In the UAV-UAV game, similar to [3], the players correspond to the set of UAVs; the action space is defined as the set of links which each UAV can delete or form; the purpose is to form a suited network graph that connects them to BS via at most one path. While in the GRs-network game, the players correspond to the set of GRs and the nodes of the network G; the action space is defined as the set of links which each node can delete or form and each GRs can form or replace; the purpose is to connect GRs with proper nodes of the network to reduce time delay in data transmission.

In the UAV-UAV game, for each UAV U_n, the purpose is to minimize its utility function $J_n(G)$ (the objective of (5)), which captures the amount of data transmitted via U_n in network G and time delay of transmitting them. In the GRs-network game, for each GRs, the purpose is to connect to one node (UAV) to transmit collected data to BS via fewer hops, the link between which should satisfy the threshold of the required communication quality $SNR_{\min}$. As for another player, the network, the purpose is to minimize its utility function $J(G)$, which is also the objective of (5). And the result of the second game is a set of links formed among different nodes (UAVs) in the network and GRs.

In the game theory, when all players act according to their best response, the game can converge to a stable state where they reach an agreement. The state is Nash equilibrium (NE) [2]. In these two games, to get to the NE, all players act based on greedy strategy, which means they make decisions to optimize their utility functions considering only the current state of the network and no future evolution. More specifically, to get to NE, players follow rules below:

(1) To form a link $e_{nn'}$ between UAV U_n and UAV U_n' ($n, n' \in \mathcal{N}, n \neq n'$), they should both agree, which is on the condition that $J_n(G-e_{np(n)}+e_{nn'}) < J_n(G)$ and $J_{n'}(G-e_{np(n)}+e_{nn'}) < J_{n'}(G)$.
(2) To delete a link $e_{nn'}$, U_n can unilaterally decide, if $J_n(G - e_{nn'}) < J_n(G)$.
(3) To form a link e_{nm} between GR GR_m ($m \in \mathcal{M}$) and one node U_n of the network G, GR_m can unilaterally decide, on the condition that $SNR_{nm} \geq SNR_{\min}$.
(4) To replace an existed link $e_{n'm}$ with a newly formed link e_{nm}, GR_m and the network G should both agree, which means $SNR_{nm} \geq SNR_{\min}$ and $J(G - e_{n'm} + e_{nn'}) < J(G)$.

3.1.2 Virtual force field. The idea of VFF is regarding a target in environments as a charged particle navigating a magnetic field. In other words, repelled by virtual forces from obstacles and attracted by virtual forces from the goal, the target can arrive at the goal while avoiding obstacles. VFF is adopted in [3] to allow a UAV to adjust its position when different UAVs are beyond the communication range. This motivates us that VFF can convert mathematical constraints to virtual forces, then update positions of UAVs. In this case, when all links are LoS, corresponding virtual forces of the problem (5) that would apply to a UAV relay are shown in Fig. 5. $\vec{F}_{re}$ is the resultant force of collision avoidance repulsive forces from different UAVs and attractive forces from GRs/BS, which can push UAVs to proper positions theoretically. Note that for the traditional VFF method, there is typically only one goal, while in this paper, there are many GRs that can be regarded as goals. Therefore, we cluster GRs based on their positions, for that GRs close to each other may share the same communication condition with high probability.

Algorithm 2 ATG-NF Algorithm

Input: $G, U_n, U_{n'}$ and $tarGRs$.
Output: G.
1: Check $J_n(G)$ and $J_{n'}(G)$.
2: **if** $e_{nn'} \notin E$ **then**
3: A resultant virtual force $\vec{F}_{re}$ is exerted to U_n to update its position; original position $x_{U_n}^{\text{old}}$ is remembered.
4: **if** $dis(U_n, c(n)) > d_A$ **then**
5: $x_{U_n} = x_{U_n}^{\text{old}}$.
6: $e_{n,GR_{U_{n'}}}$ can replace $e_{n',GR_{U_{n'}}}$, if $SNR_{n,GR_{U_{n'}}} > SNR\text{min}$ and $J(G - e_{n',GR_{U_{n'}}} + e_{n,GR_{U_{n'}}}) < J(G)$.
7: **end if**
8: **if** $c(n)$ not exist or $dis(U_n, c(n)) \leq d_A$ **then**
9: Form links e_{nm} ($GR_m \in tarGRs$) if $SNR_{nm} > SNR\text{min}$.
10: **if** $J_n(G-e_{np(n)}+e_{nn'}) < J_n(G)$ and $J_{n'}(G-e_{np(n)}+e_{nn'}) < J_{n'}(G)$ **then**
11: Form $e_{nn'}$ and replace $e_{np(n)}$.
12: **else**
13: $x_{U_n} = x_{U_n}^{\text{old}}$.
14: Delete links e_{nm} formed in line 9.
15: **end if**
16: **end if**
17: **end if**
18: **if** $e_{nn'} \in E$ **then**
19: delete $e_{nn'}$ if $J_n(G - e_{nn'}) < J_n(G)$;
20: $e_{n,GR_{U_{n'}}}$ can replace $e_{n',GR_{U_{n'}}}$, if $SNR_{n,GR_{U_{n'}}} > SNR\text{min}$ and $J(G - e_{n',GR_{U_{n'}}} + e_{n,GR_{U_{n'}}}) < J(G)$;
21: **end if**

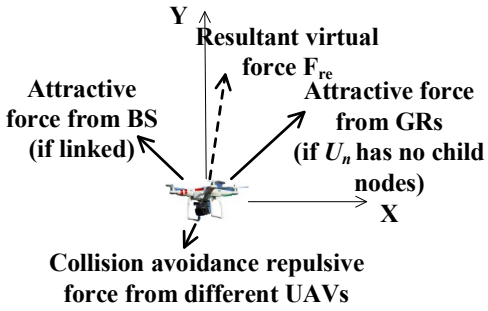

Figure 5: Illustration of virtual forces that would apply to a UAV relay.

3.1.3 Algorithm design. Based on the two games and VFF, our proposed algorithm is given in Algorithm 2. Input parameters U_n, $U_{n'}$ and $tarGRs$ are chosen in line 2-4 in Algorithm 1, while UAVs with less child UAVs are assigned with higher priority. In Algorithm 2, we have two situations: link $e_{nn'}$ does not exist (in line 2-17) and the other (in line 18-21). When link $e_{nn'}$ does not exist, a resultant virtual force is exerted to U_n to establish a temporarily

communication link with $U_{n'}$ and make it closer to goal GRs. Then compare the Euclidean distance between the updated U_n and its child UAV $dis(U_n, c(n))$ and the maximum distance between any two UAVs satisfying the threshold of communication quality $d_A = \sqrt[\beta]{\frac{\Phi(t_{nn'})P_n}{SNR_{\min}N_0B\Psi^{LoS}}}$. If U_n in the newly position is disconnected from its child nodes, U_n should be returned to its original position. Then, present network and $GR_{U_{n'}}$ (linked GRs with $U_{n'}$) engage in the GRs-network game (line 4-7). If U_n has no child node or $dis(U_n, c(n))$ is within the maximum distance d_A, U_n and $U_{n'}$ engage in the UAV-UAV game while GRs in $tarGRs$ and G engage in the GRs-network game (line 9-15). On the other hand, if link $e_{nn'}$ exists, U_n and $U_{n'}$ engage in the UAV-UAV game while GRs in $GR_{U_{n'}}$ and G engage in the GRs-network game (line 19-20). At last, we can get network G with updated links and node positions.

3.2 Communication Quality-Aware UAV Placement Problem

Based on the network topology resulted from the ATG-NF algorithm, the problem (5) can be transformed as

$$\begin{aligned} \min_{x_{Un}, n\in\mathcal{N}} \quad & J = -\sum_{n\in\mathcal{N}}\sum_{m\in\mathcal{M}}\Phi(t_{nm})A_m \\ s.t. \quad & d_{nn'} \le \sqrt[\beta]{\frac{\Phi(t_{nn'})P_n}{SNR_{\min}N_0B\Psi^{LoS}}}, \\ & d_{no} \le \sqrt[\beta]{\frac{\Phi(t_{no})P_n}{SNR_{\min}N_0B\Psi^{LoS}}}, \\ & dis(U_n, U_{n'}) > d_{\text{safe}}, \\ & \frac{\Phi(t_{nm})P_n}{N_0Bd_{nm}{}^{\beta}\Psi_{nm}} \ge SNR_{\min}, \forall n, n', m, n \ne n'. \end{aligned} \tag{6}$$

For that Ψ_{nm} is a step function of x_{Un}, the problem (6) is a multi-objective non-convex optimization problem, which optimizes positions of UAVs to transmit more data while satisfying the communication quality. Due to topology and communication quality constraints, the change of position of one UAV would affect positions of its directly linked UAVs, e.g., one UAV moving to the best position may make child nodes of it disconnect with the network. Note that in nature, the orientation of tree root can decide the growth orientation of the tree. Similarly, in our tree-structure network, positions of UAVs closer to the root (BS) can influence the GRs that the network can link. Therefore, the basic idea of the CQA-UP algorithm is to assign the most important weight to UAVs closer to BS, and the assigned weights fall as the UAVs locate further from the BS. In this way, we transform the multi-objective optimization problem into single-objective optimization problem by optimizing the UAVs closer to BS first and then their child UAVs.

Note that when UAV flying height is fixed, the closer the UAV moves to the GR, the more likely the link between them has LoS propagation [1], then satisfies the required communication quality. Therefore the objective function of (6) can be approximated as minimizing the distance between U_n and center of $tarGRs$ ($J = dis(U_n, cen(tarGRs))$). In this case, if the value of Ψ_{nm} is definite, (6) is a convex problem, which therefore can be easily solved by methods like interior point method. By utilizing LoS condition-based division [19], we can make the value of Ψ_{nm} definite. In detail, by regarding the radio propagation as the ray optics propagation, we can divide the domain of x_{U_n} into areas with LoS ($D^{LoS}_{U_n}$) and NLoS propagation ($D^{NLoS}_{U_n}$) when U_n communicates with linked GRs separately. In $D^{LoS}_{U_n}$, the value of Ψ_{nm} is definite. Since $D^{LoS}_{U_n}$ could be concave with high probability, we next divide it into several convex subdomains, in which subproblems of (6) are convex and can be easily solved. The minimum solution among these subproblems corresponds to the optimal solution, the optimal position of the optimized UAV.

Algorithm 3 CQA-UP Algorithm

Input: ρ_n, obs, $tarGRs$ and $\mathcal{N}$.
Output: Positions of UAVs in $\rho_n = \{U_{l1}, U_{l2}, ..., U_{ln}\}$.

1: **for** each $i \in [l_1, l_n]$ **do**
2: $U_{\text{oth}} = \mathcal{N} - U_i$.
3: $U_\eta = (\mathcal{N} - \rho_n) \cap c(i)$.
4: **if** $U_\eta == \varnothing$ **then**
5: $D_{x_{U_i}} = O(x_{p(i)}, d_A) - O(x_{U_{\text{oth}}}, d_{safe})$.
6: **else**
7: $D_{x_{U_i}} = O(x_{p(i)}, d_A) \cap O(x_{U_\eta}, d_A) - O(x_{U_{\text{oth}}}, d_{safe})$.
8: **end if**
9: Define the jth linked GRs with U_i as $GR_{U_i,j}$.
10: Divide the flyable area of U_i into $D^{LoS}_{GR_{U_i,j}}$ and $D^{NLoS}_{GR_{U_i,j}}$ when U_i communicates with $GR_{U_i,j}$, according to obs and $x_{GR_{U_i,j}}$.
11: $S_j = S(D_{x_{U_i}} - D^{NLoS}_{GR_{U_i,j}})$.
12: Sort S_j in descending order as $S_{k_1}, S_{k_2}, ..., S_{k_j}$.
13: **for** each $K \in [k_1, k_j]$ **do**
14: **if** $S(D_{x_{U_i}} - D^{NLoS}_{GR_{U_i,K}}) == 0$ **then**
15: Delete link between U_i and $GR_{U_i,K}$.
16: **else**
17: $D_{x_{U_i}} = D_{x_{U_i}} - D^{NLoS}_{GR_{U_i,K}}$.
18: **end if**
19: **end for**
20: Divide domain $D_{x_{U_i}}$ into several convex subdomains $D^{\varepsilon}_{x_{U_i}}$.
21: In subdomains $D^{\varepsilon}_{x_{U_i}}$, subproblem (6) are convex problems, and optimal solutions among these subproblems are $x^{\varepsilon*}_{U_i}$ and $J^{\varepsilon*}_{U_i}$.
22: $J^*_{op} = min\{J^{\varepsilon*}_{U_i}\}$ and $x^*_{U_i}$ is the corresponding $x^{\varepsilon*}_{U_i}$.
23: **end for**

The entire algorithm is summarized in Algorithm 3. Input parameter ρ_n is the set of UAVs to be optimized, which is chosen in line 8 in Algorithm 1. In Algorithm 3, UAVs are optimized from the ones closer to BS. For each UAV i to be optimized, U_{oth} is the set of UAVs apart from itself, while U_η is the set of its child UAVs except UAVs to be optimized. In line 2-8, we have the domain of x_{U_i} satisfying the first three constraints in (6). To make the value of the shadow fading component definite, $D^{NLoS}_{GR_{U_i,j}}$ should both be removed from $D_{x_{U_i}}$. In case there are no area left, the link with the GR that leads to the least left area would be deleted, until there are some areas left (line 11-19). Then, following the LoS condition-based division, we can get the newly positions of UAVs in ρ_n.

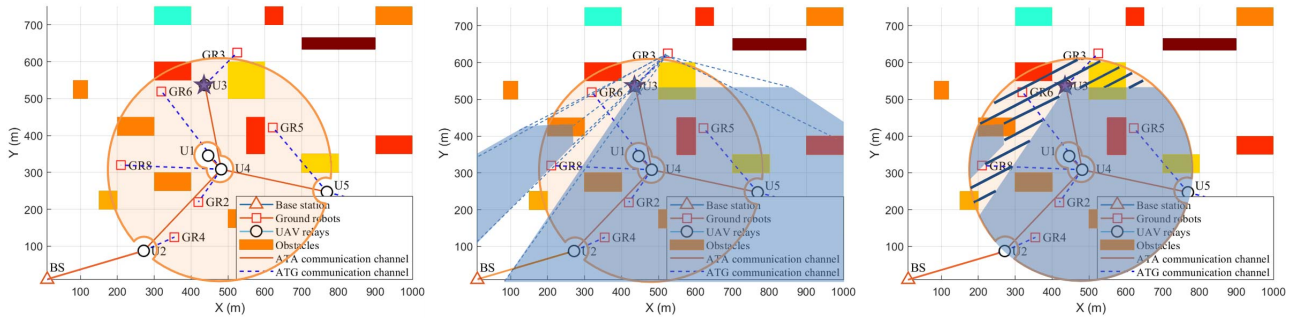

(a) (b) (c)

Figure 6: Diagrammatic sketch of the CQA-UP algorithm. The star represents the UAV to be optimized. (a) Orange circle region is the domain of x_{U_3} satisfying the first three constraints in (6). (b) Blue regions are areas with NLoS propagations when U_3 communicates with linked GRs (GR_3). (c) The left orange shadow region is the final domain of x_{U_3}, which can make the value of the shadow fading component definite.

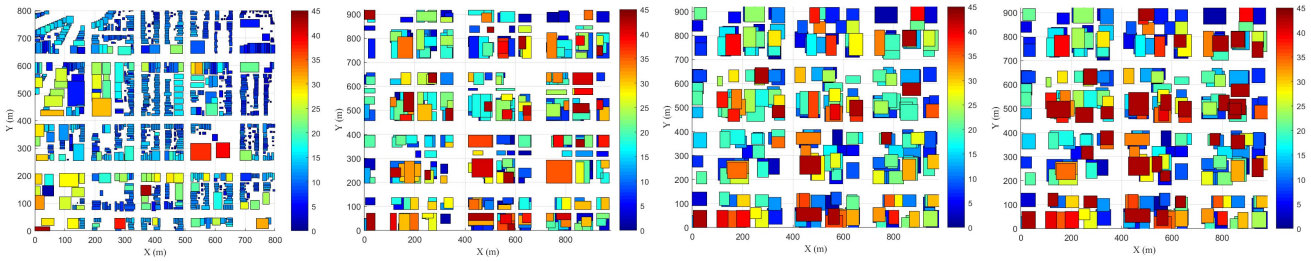

(a) Suburban (0.25, 1265, 10) **(b) Urban (0.37, 461, 18)** **(c) Dense urban (0.4966, 310, 20)** **(d) Urban high-rise (0.4966, 310, 45)**

Figure 7: Four typical types of urban environments recommended by ITU-R, followed by parameters (a, b, c). The original data of these environments are either obtained from real-world datasets (the USGS database: http://ngmdb.usgs.gov) or adapted from existing works[6].

An example is visualized in Fig. 6, where $\rho_3 = \{U_2, U_4, U_3\}$, U_3 is the UAV to be optimized, and $U_\eta = \emptyset$. $D_{x_{U_3}}$ after line 8 in Algorithm 3 is shown in orange circle region in Fig. 6a, $D^{NLoS}_{GR_{U_3,1}}$ is shown in blue regions in Fig. 6b, and the final domain of x_{U_3} is shown in orange shadow region in Fig. 6c.

4 NUMERICAL RESULTS

In this section, we present our simulations to verify the validity and task performance of the proposed mUP method with different numbers of UAVs in different types of urban environments with obstacles by comparing it with the other two methods. Then we show how the system is used in successive time intervals in surveillance scenarios. Besides, we analyze the robustness of the mUP method towards terrain measurement error since maps of environments may be imprecise due to limitations of mapping technologies or in post-disaster scenarios.

For simulations, we consider four different Manhattan-like 1 km by 1 km urban environments with trees and buildings ranging between 5-45 meters height. As shown in Fig. 7, we assume obstacles like trees and buildings are convex and simplify them into cuboids.

Table 2: System parameters

Parameters	Values
Transmit power (P)	30 dBm
Bandwidth (B)	5 MHz
Noise power spectral density (N_0)	-90 dBm/Hz
SNR threshold (SNR_{min})	-4 dB
(μ_{LoS}, μ_{NLoS})	(0.1,21)
Path loss (β)	2.5
Heights of BS and UAVs (h_{BS}, h_U)	45 m, 50 m
Collision avoidance threshold (d_{safe})	10 m

As recommended by The International Telecommunication Union (ITU-R) [9], the ratio of built-up area (a), the mean number of buildings per unit area (b), and building height distribution-related parameter (c) are three empirical parameters that can describe environments. According to these parameters, four environments in Fig. 7 can represent four typical types of urban environments: suburban, urban, dense urban and urban high-rise.

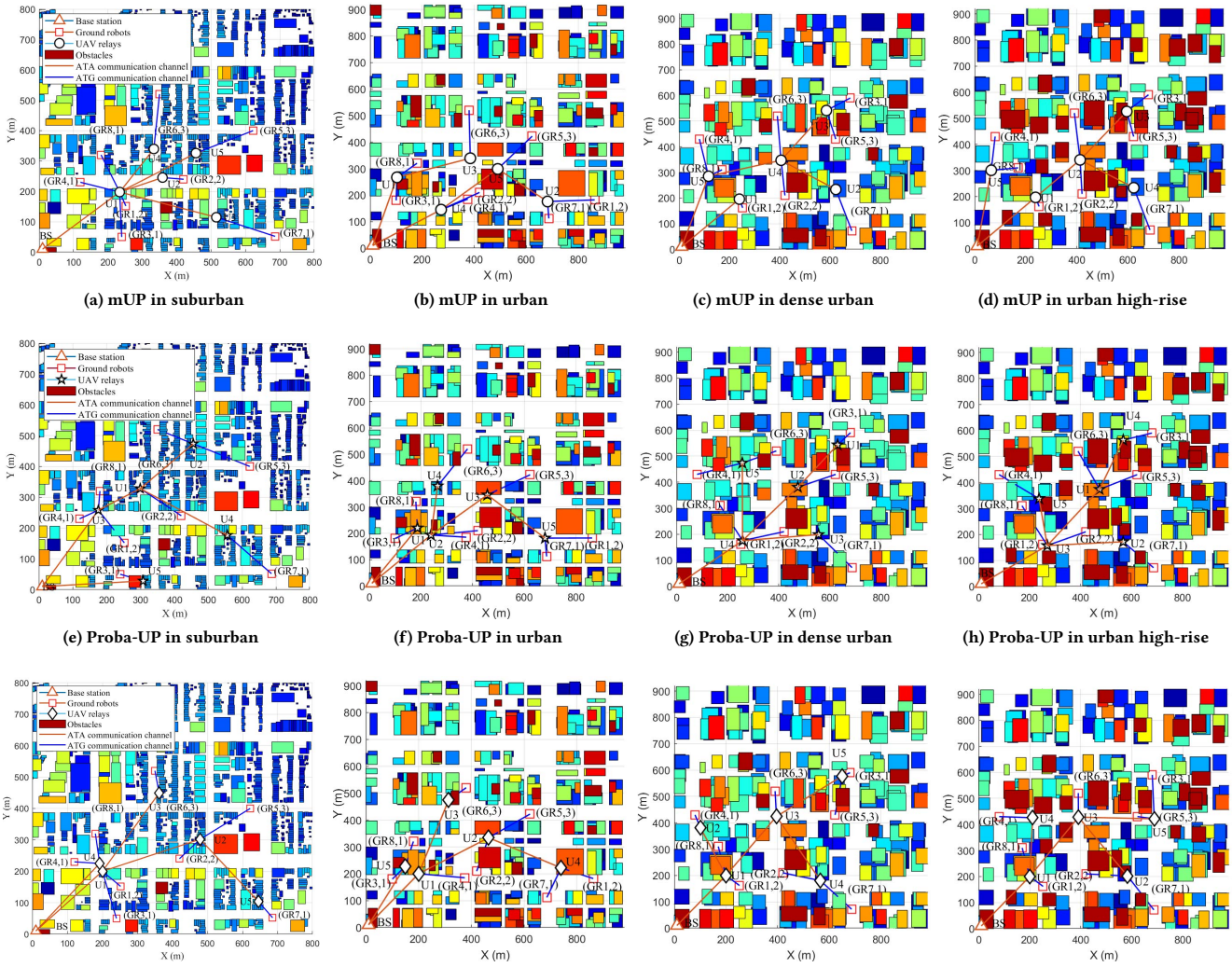

(a) mUP in suburban (b) mUP in urban (c) mUP in dense urban (d) mUP in urban high-rise

(e) Proba-UP in suburban (f) Proba-UP in urban (g) Proba-UP in dense urban (h) Proba-UP in urban high-rise

(i) VFF-UP in suburban (j) VFF-UP in urban (k) VFF-UP in dense urban (l) VFF-UP in urban high-rise

Figure 8: The placements of 5 UAVs optimized by the proposed mUP method (shown by circle lines), Proba-UP method (shown by pentagram lines), and VFF-UP method (shown by diamond lines) separately in four different types of urban environments in top viewpoint. The network composed of 5 UAVs is initialized as a star network, where each UAV connects to the BS via a direct link. There are 8 GRs and (GRm, a_m) means the m-th GR collects a_m times as much as a_0 (Mbits) data. The value of a_0 depends on specific tasks.

The main simulation parameters are summarized in Table 2. GRs are spread at ground level in predefined ways according to their tasks. UAV flying heights are set to 50 meters to avoid collision with any building while maintaining LoS propagation with the BS. As for the UAV-to-GRs links, we consider both LoS and NLoS propagation scenarios, relevant propagation parameters that correspond to existing literature models for a fair comparison [3, 11]. Besides, the bandwidth per UAV is the same since we adopt TDMA. All statistical results are averaged over 500 independent runs.

4.1 Superiority of the mUP Method in Task Performance

In this subsection, we simulate the scenario described in Section 2 in four typical types of urban environments. And we compare our proposed mUP method with following baselines.

- **UAVs placement using probabilistic LoS channel model (Proba-UP)**: the probabilistic LoS channel model is the widely-used statistical communication channel model in existing research when dealing with environments with obstacles [3, 8, 17, 18]. Since existing works either considered the phone users and cared little about the precise positions of

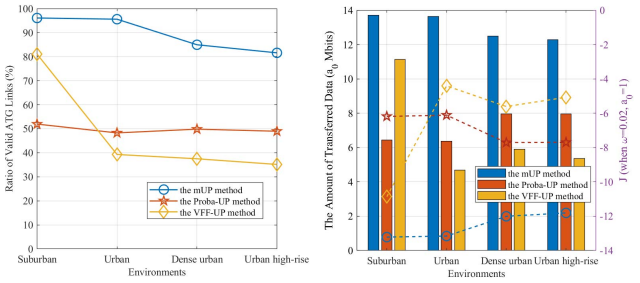

(a) The ratio of valid ATG links (b) Value of objective J and the amount of transferred data via the network

Figure 9: With the same sets of Fig. 8, valid link ratios, objective J and the amount of transferred data via the network formed by three methods in four types of urban environments. ATG links satisfying the threshold of SNR are assumed to be valid. And the "ratio of valid ATG links" is the ratio of valid links to the number of GRs. The total amount of the data collected by 8 GRs are $14a_0$ (Mbits).

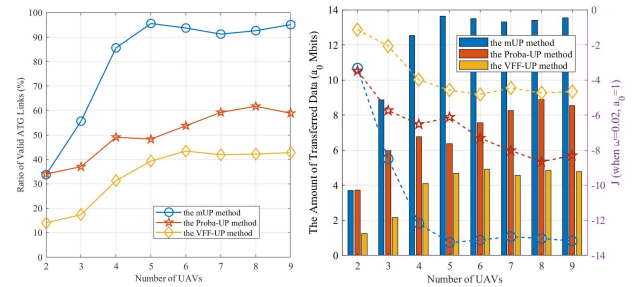

(a) The ratio of valid ATG links (b) Value of objective J and the amount of transferred data via the network

Figure 10: With the same set of GRs in Fig. 8b, valid link ratios, objective J and the amount of transferred data via the network formed by three methods. The number of UAVs ranges from 2-9.

GRs or based on communication models like free-space path loss model without reckoning on the impact of obstacles, their methods cannot be applied to this scenario directly. Therefore, in this paper, we implement it by substituting the shadow fading component with the probabilistic shadow fading component Ψ_{ij}^{proba}:

$$\begin{aligned} \Psi_{ij}^{proba} &= P_{ij}^{LoS}\mu_{ij}^{\text{LoS}} + (1 - P_{ij}^{LoS})\mu_{ij}^{\text{NLoS}}, \\ P_{ij}^{LoS} &= 1/(1 + C\exp(-D[\theta - C])). \end{aligned} \tag{7}$$

The probability of one link e_{ij} having an LoS propagation (P_{ij}^{LoS}) is related to the distribution of obstacles (C, D) and the elevation angle between transmitter and receiver (θ) [1]. (C, D) can be obtained from (a, b, c) according to [1]. In this case, the problem (6) can be transformed into a convex problem, which methods like the interior point method can solve.

- **UAVs placement using virtual force field (VFF-UP)**: Noted that using the proposed ATG network formation algorithm alone, we can theoretically get the proper placement of UAVs. Apart from virtual forces shown in Fig. 5, we take the repulsive forces from obstacles into consideration in this method. Besides, we implement this method by carefully adjusting the virtual force attractive coefficient parameters according to information of environments.

As shown in Fig. 8, in top viewpoint, we compare the placements of UAVs optimized separately by mUP method (Fig. 8a- Fig. 8d), Proba-UP method (Fig. 8e- Fig. 8h) and VFF-UP method (Fig. 8i-Fig. 8l) in four types of environments. Overall, we can see that all ATG communication links deployed by mUP method are LoS, while ATG links deployed by Proba-UP method and VFF-UP method have both LoS and NLoS propagations (e_{U_1,GR_8} in Fig. 8f and e_{U_4,GR_1} in Fig. 8j for instance). This should owe to the CQA-UP algorithm, which utilizes the information of obstacles and optimizes positions of UAVs to ensure the required communication quality. As for UAVs placements optimized by Proba-UP method, UAVs tend to move to places with higher probability of having LoS propagations, on the condition that obstacles are evenly distributed in environments. It turns out that this does not work well in real-world dataset, in which obstacles are usually randomly distributed. When it comes to UAVs placements optimized by VFF-UP method, UAVs are usually deployed close to positions above no obstacles. This is because in VFF-UP method, UAVs are pushed by resultant forces of attractive forces from GRs/BS, collision avoidance repulsive forces from other UAVs and all obstacles in environments. However, UAV in positions above no obstacles cannot guarantee the UAV-to-GRs links are LoS, which is why our proposed mUP method contains ATG-NF algorithm (similar to VFF-UP method), as well as CQA-UP algorithm.

In Fig. 9, we quantitatively compare the ratio of valid ATG links, the objective J, and the amount of transferred data via the network deployed by the mUP method, Proba-UP method, and VFF-UP method in four different types of urban environments. In Fig. 9a, we can see that the ratio of valid ATG links of these three method are in line with the analysis, where ratios of the proposed mUP method are always more than 80%, ratios of Proba-UP method are around 50%, and ratios of VFF-UP method steadily drop with environments becoming crowded. Similarly, in Fig. 9b, we can see that values of objective J resulting from the mUP method are the minimum, and the network formed by the mUP method can transfer up to 2 times and 3 times the amount of data as much as that of the Proba-UP method and the VFF-UP method.

In addition, we also analyze the influence of different numbers of UAVs on the ratio of valid ATG links, the objective J, and the amount of transferred data in Fig. 10. Overall, the results trend illustrates that ratios and the amount of data increase with the UAVs number until they reach their peak value in all methods, and the trend of J is on the contrary. This is because that UAVs at first are too few to link all remote GRs, then GRs are linked with the increase of the UAVs. Besides, the final values of ratios, J, and the amount of data are consistent with previous observations in Fig. 9.

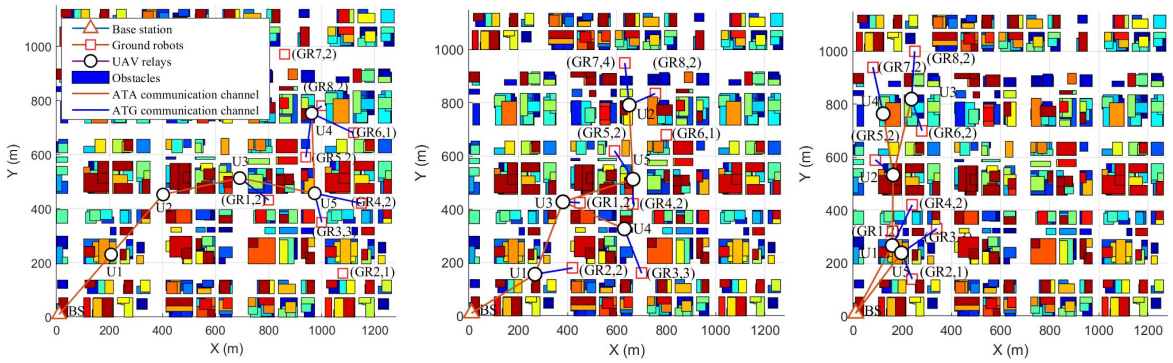

(a) Time interval one (b) Time interval two (c) Time interval three

Figure 11: Three networks resulting from the proposed mUP method in three successive time intervals, which shows how the proposed method is used in successive task executions in surveillance scenarios. The initial state of the network in (a) is the star network, and the resulted network in present time interval is the initial state of the network in next time interval.

In conclusion, these observations show the superiority of the mUP method in improving communication quality and task performance.

4.2 Successive Task Executions in Surveillance Scenarios

In this subsection, we show how the proposed mUP method is used in successive task executions in surveillance scenarios. In successive time intervals, each GR first collects data in a predefined trajectory according to the surveillance areas assigned to it, then rests on a predefined position to transmit data to the BS via UAVs. For example, from time interval one to time interval two, GRs collect data while move from positions shown in Fig. 11a to positions shown in Fig. 11b, then rest on positions shown in Fig. 11b to transmit data.

In Fig. 11a, GRs are at remote positions, and UAVs form a line-structure network to extend the communication range. We can see that all links are LoS. GR_7 and GR_2 are unlinked since they are too far and have relatively small amount of data. And the collected data will be saved until being transmitted. When GRs move to positions in Fig. 11b, the network changed to a tree-structure one to reduce time delay in data transmission. And data collected by GR_7 and GR_2 are transmitted into the BS in this time interval. GR_2 is unlinked, for that links connecting it to UAVs are significantly obstructed by surrounding high buildings. As GRs move more closer in Fig. 11c, the topology of the network has changed to another tree-structure one. We can see that all GRs are linked while all links are LoS.

4.3 Robustness of the mUP method towards Terrain Measurement Error

The proposed mUP method is based on accurate maps of environments, which can be obtained by digital elevation model (DEM) data or technologies like oblique photography. However, measurement errors or environmental damages caused by disaster (are collectively called "terrain measurement errors" in this paper) may make the map of environments imprecise. Therefore, in this subsection, we analyze the robustness of the proposed method towards terrain measurement error.

In this paper, obstacles are simplified into cuboids, which can be represented with the following parameters: height, location, length and width. We get an **imprecise environment** by adding terrain measurement errors to obstacles in the **accurate environment** separately. The terrain measurement error ratio [19] is used to make it quantitative. For example, 20% of terrain measurement error ratio means 15% $\sim$ 20% or -20% $\sim$ $-$15% random terrain measurement errors add to each obstacle in the accurate environment. As for the validation, the proposed method is firstly applied in the imprecise environment, then the result of which is validated in the accurate environment. If produced UAVs-to-GRs links are still LoS in the accurate environment, they are assumed to be valid. And the validness ratio is the ratio of the number of valid links to that of all UAV-to-GRs links. With the same positions set of GRs in Fig. 8, validness ratios of mUP method for different terrain measurement error ratios in different obstacle-related parameters in four types of urban environments are shown in Fig. 12.

Overall, we can see that the ratio of validness falls as the terrain measurement error ratio increases. Besides, sorting these parameters by influence on validness ratio in descending order, they are as: all of them, location, length/width and height. In addition, we can see there are some fluctuations in Fig. 12, which is because some random measurement errors such as the bigger width or positional error of obstacles may not make the UAV-to-GRs links blocked and therefore not influence the validness of links. When the terrain measurement error ratio in location/all parameters is bigger than 5% in all environments, the ratio of validness of the mUP method drops to around 50%, which is close to the result of the Proba-UP method (refer to Fig. 9a). In this case, the result of the mUP method is considered to be distrusting. As for the length/width and height parameters, the ratio of validness of the proposed method remains more than 60% in all environments, the result of which means at least 60% UAV-to-GRs links are LoS and can be considered as functional. In addition, validness ratios in suburban, urban, dense urban and urban high-rise environments are above 60%, 50%, 45% and 40%.

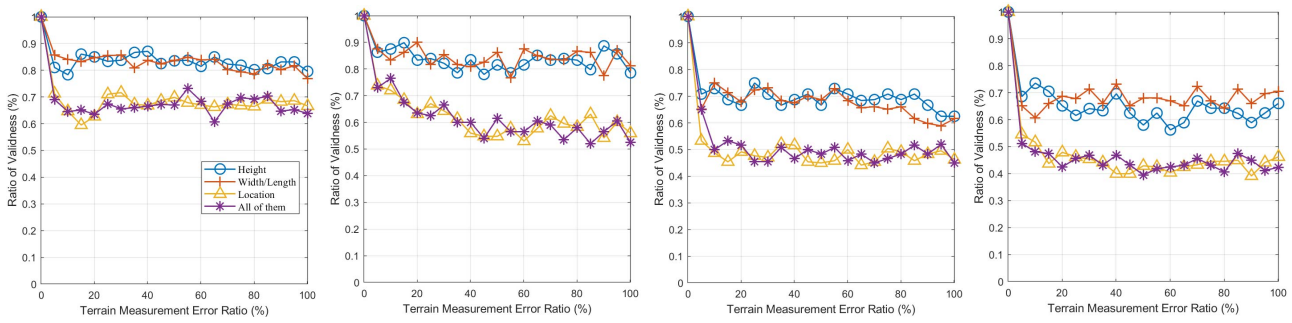

(a) Suburban (b) Urban (c) Dense urban (d) Urban high-rise

Figure 12: The validness ratio of resulted links for different terrain measurement error ratios in different obstacle-related parameters in different types of urban environments, which illustrates the robustness of the proposed mUP method towards terrain measurement error. Placements of UAVs produced in imprecise environments are validated in original accurate environments. If UAV-to-GRs ATG links produced in the imprecise environment are still LoS in the original accurate environment, they are assumed to be valid.

Based on all these observations, we can see that the proposed mUP method is tolerant to shape measurement errors (measurement errors in length/width or height parameters), but sensitive to location measurement errors (measurement errors in location parameters). Besides, note that in post-disaster scenarios, shape measurement errors may occur with a higher probability when buildings collapse. In this case, we may conclude that as far as the measurement error ratio is below 5%, the proposed method can be regarded as functional and robust. In addition, the robustness of the mUP method performs better in suburban and urban environments, which are relatively sparse and have fewer tall buildings.

5 CONCLUSION

In this paper, we considered urban surveillance and post-disaster scenarios, where backhaul access was either unavailable or limited in capacity due to the existence of obstacles. A UAV-enabled wireless multi-hop network was deployed to serve several task-oriented GRs to transmit their collected data to a remote BS. Considering the impact of obstacles, we proposed an mUP method to form a network to transfer more data collected by GRs and minimize the time delay in data transmission. We tackled this problem by reconstructing it into the ATG-NF subproblem and the CQA-UP subproblem, and solving them alternatively. By designing the UAV-UAV game and the GRs-network game and incorporating VFF, we solved the first subproblem to get the topology deployment of the network. Then by assigning different weights to different UAVs and using LoS condition-based division, we transform the second multi-objective optimization subproblem into single-objective optimization convex subproblems. Then we got positions of UAVs where communication qualities are satisfied.

Simulation results have shown that the proposed method yields significant performance gains in communication quality and task execution compared with the Proba-UP method and the VFF-UP method in four typical types of urban environments or with different numbers of UAVs. Besides, results show that the mUP method can cope with successive task executions. In addition, we also analyze the robustness of it towards terrain measurement error. Results show that so far as the location measurement error ratio is below 5%, which can be satisfied by most mapping technologies, the mUP method can be regarded as functional and robust. Moreover, the robustness of the mUP method performs better in environments that are sparser and have fewer tall buildings.

In our future work, we will consider a more realistic scenario with an online-measured communication channel and 3D deployment of UAVs, then evaluate the mUP method in real experiments. Besides, homogeneous quadrotors are considered in this paper, how to adapt to fixed-wing UAVs or heterogeneous UAVs can be investigated. Moreover, treating ground robots as relays is another promising solution, which introduces the interesting optimization problem of deploying UAVs and ground robots to maximize task performance efficiency.

ACKNOWLEDGMENTS

This work was supported by the National Natural Science Foundation of China (No. 91948303).

REFERENCES

[1] A. Al-Hourani, S. Kandeepan, and S. Lardner. 2014. Optimal LAP Altitude for Maximum Coverage. *Wireless Communications Letters IEEE* 3, 6 (2014), 569–572.
[2] Bacci, G., Lasaulce, S., Saad, W., Sanguinetti, and L. 2016. Game Theory for Networks: A tutorial on game-theoretic tools for emerging signal processing applications. *Signal Processing Magazine, IEEE* 33, 1 (2016), 94–119.
[3] U. Challita and W. Saad. 2017. Network Formation in the Sky: Unmanned Aerial Vehicles for Multi-Hop Wireless Backhauling. In *GLOBECOM 2017 - 2017 IEEE Global Communications Conference*. 1–6.
[4] U. Challita, W. Saad, and C. Bettstetter. 2018. Deep Reinforcement Learning for Interference-Aware Path Planning of Cellular-Connected UAVs. In *2018 IEEE International Conference on Communications (ICC 2018)*. 1–7.
[5] Junting Chen and David Gesbert. 2017. Optimal positioning of flying relays for wireless networks: a LOS map approach. In *2017 IEEE international conference on communications (ICC)*. IEEE, 1–6.
[6] Junting Chen and David Gesbert. 2019. Efficient local map search algorithms for the placement of flying relays. *IEEE Transactions on Wireless Communications* 19, 2 (2019), 1305–1319.
[7] Omid Esrafilian, Rajeev Gangula, and David Gesbert. 2020. Autonomous UAV-aided Mesh Wireless Networks. In *IEEE INFOCOM 2020 - IEEE Conference on*

Computer Communications Workshops (INFOCOM WKSHPS). 634–640.

[8] P. Foroughi, H. Beyranvand, M. Gagnaire, and S. A. Zahr. 2020. User Association in Hybrid UAV-cellular Networks for Massive Real-time IoT Applications. In *IEEE INFOCOM 2020 - IEEE Conference on Computer Communications Workshops (INFOCOM WKSHPS)*. 243–248.

[9] ITU-R. 2003. Rec. P.1410-2 Propagation Data and Prediction Methods for The Design of Terrestrial Broadband Millimetric Aadio Access Systems. *P Series, Radiowave propagation* (2003).

[10] M. Jaber, M. A. Imran, R. Tafazolli, and A. Tukmanov. 2017. 5G Backhaul Challenges and Emerging Research Directions: A Survey. *IEEE Access* 4 (2017), 1743–1766.

[11] Pawel Ladosz, Hyondong Oh, Gan Zheng, and Wen-Hua Chen. 2019. A hybrid approach of learning and model-based channel prediction for communication relay UAVs in dynamic urban environments. *IEEE Robotics and Automation Letters* 4, 3 (2019), 2370–2377.

[12] P. Li and J. Xu. 2018. Placement Optimization for UAV-Enabled Wireless Networks with Multi-Hop Backhauls. *Journal of Communications and Information Networks* (2018), 64–73.

[13] M. Mozaffari, W. Saad, M. Bennis, Y. H. Nam, and M. Debbah. 2019. A Tutorial on UAVs for Wireless Networks: Applications, Challenges, and Open Problems. *IEEE Communications Surveys and Tutorials* (2019), 2334–2360.

[14] Arjun Muralidharan and Yasamin Mostofi. 2021. Communication-aware robotics: Exploiting motion for communication. *Annual Review of Control, Robotics, and Autonomous Systems* 4 (2021), 115–139.

[15] S. A. R. Naqvi, S. A. Hassan, H. Pervaiz, and Q. Ni. 2018. Drone-Aided Communication as a Key Enabler for 5G and Resilient Public Safety Networks. *IEEE Communications Magazine* 56, 1 (Jan 2018), 36–42.

[16] Luis Ramos Pinto and Luis Almeida. 2018. A robust approach to TDMA synchronization in aerial networks. *Sensors* 18, 12 (2018), 4497.

[17] W. Saad, Z. Han, T Başar, M. Debbah, and A Hjørungnes. 2012. Network Formation Games Among Relay Stations in Next Generation Wireless Networks. *IEEE Transactions on Communications* 59, 9 (2012), 2528–2542.

[18] N. Xing, Q. Zong, B. Tian, L. Dou, and Q. Wang. 2018. Network Formation Game for Routing in Unmanned Aerial Vehicle Networks. In *2018 IEEE/CIC International Conference on Communications in China (ICCC)*. 704–708.

[19] Sining Yang, Dianxi Shi, Yingxuan Peng, Wei Qin, and Yongjun Zhang. 2021. Joint Communication-Motion Planning for UAV Relaying in Urban Areas. In *2021 18th Annual IEEE International Conference on Sensing, Communication, and Networking (SECON)*. 1–9.

[20] Yong Zeng, Rui Zhang, and Teng Joon Lim. 2016. Wireless communications with unmanned aerial vehicles: opportunities and challenges. *IEEE Communications Magazine* 54, 5 (May 2016), 36–42.

[21] S. Zhang, Y. Zeng, and R. Zhang. 2018. Cellular-Enabled UAV Communication: A Connectivity-Constrained Trajectory Optimization Perspective. *arXiv* 67, 3 (2018), 2580–2604.